

Fancy Bioisosteres: Novel Paracyclophane Derivatives As Super-Affinity Dopamine D3 Receptor Antagonists

Karin Schlotter, Frank Boeckler, Harald Hübner, and Peter Gmeiner*

Department of Medicinal Chemistry, Emil Fischer Center, Friedrich Alexander University, Schuhstrasse 19, D-91052 Erlangen, Germany

Received February 8, 2006

The exploration of the chemical diversity space depends on the discovery of novel bioisosteric elements. As a continuation of our project on bilayered arene surrogates, we herein report on [2.2]paracyclophane-derived dopamine D3 receptor antagonists of type **4** and **6**. For the most promising test compound **6a**, bearing a 2-methoxyphenyl substituent, a stereocontrolled preparation was performed when the planar chirality of enantiomers (*R*)-**6a** (FAUC 418) and (*S*)-**6a** caused a considerable differentiation of D3 binding, which is indicated by K_i values of 0.19 and 3.0 nM, respectively. Functional experiments showed D3 antagonist properties for the paracyclophane derivatives of type **6**. To elucidate putative bioactive low-energy conformations, DFT-based studies including the calculation of diagnostic magnetic shielding properties were performed. An 89% increase in volume for the [2.2]paracyclophane moiety compared to that of the monolayered benzofurane of lead compound **3b** indicates higher plasticity of GPCR binding regions than usually expected.

Introduction

To optimize potency and selectivity or to improve the overall ADME profile of lead compounds, medicinal chemists have widely pursued the strategy of bioisosteric replacement.¹ The concept of bioisosterism refers to compounds or substructures of compounds that share similar shapes, volumes, electronic distributions, and physicochemical properties, which together effect similar biological activities. In addition to the successful introduction of enynes and endiynes into dopaminergics,² we found out that hitherto unknown [2.2](4,7)indoloparacyclophanes of type **2** can be used as double-layered aryl bioisosteres of the highly selective D4 receptor ligand **1** (FAUC 213), demonstrating that sterically demanding paracyclophane derivatives are capable of approaching and recognizing transmembrane receptor binding sites (Chart 1).³ Exploring the chemical diversity space of bioactive compounds, we discovered metallocene-derived bioisosteres of type **5** (FAUC 378) as exceptionally strong-binding G-protein receptor ligands when our studies were built on the naphthalene-derived D3 receptor partial agonist **3a** (BP 897) and its benzofuranyl congener **3b**.^{4,5} Changing D3 selectivity of the monolayered lead compounds into a D4 preferential binding pattern, the ferrocenyl- and ruthenocenyl-carboxamides investigated displayed not only subnanomolar binding affinity but also D3 and D4 agonist properties. Conceptual hybridization of the above-mentioned lead compounds directed us to the double-layered target molecules of type **4** and **6**, when a [2.2]paracyclophane moiety was envisaged to replace the benzofurane and metallocene units of dopaminergics **3b** and **5**, respectively. We herein present chemical synthesis of novel types of paracyclophanes and their biological evaluation for GPCR ligand binding involving dopamine D1, D2_{short}, D2_{long}, D3 and D4, serotonin 5-HT_{1A} and 5-HT₂, and adrenergic α_1 -receptors. Because we were intrigued by the question of whether the bilayered cyclophane systems will behave as agonists or antagonists, functional experiments were performed. To gain a better understanding of the steric,

electrostatic, and conformational properties of the novel bioisosteres, computational investigations were done involving the comparison of DFT-based calculations with NMR-derived experimental data.

Results and Discussion

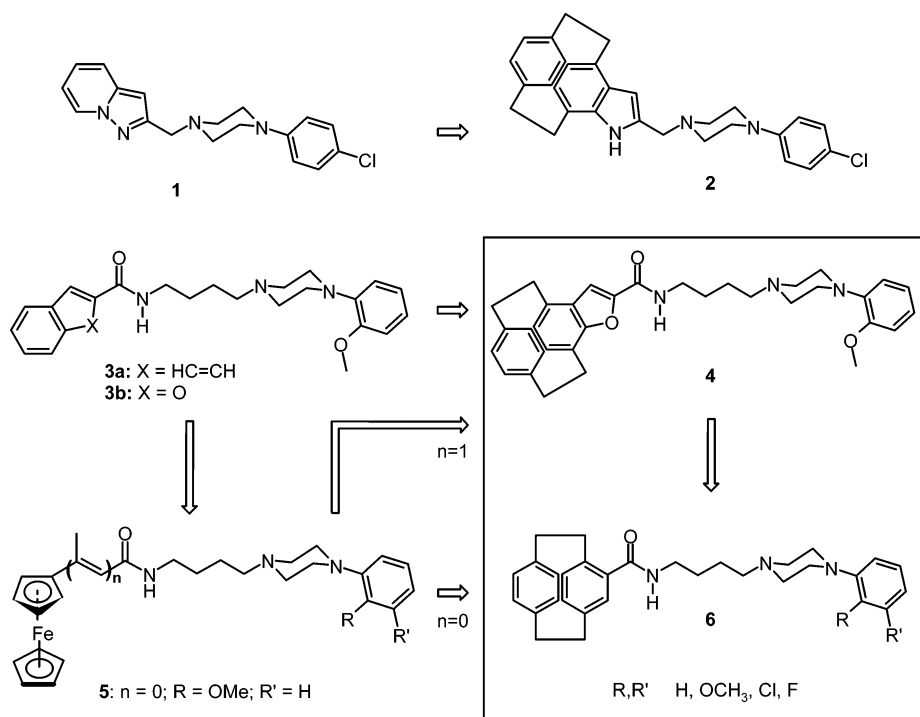
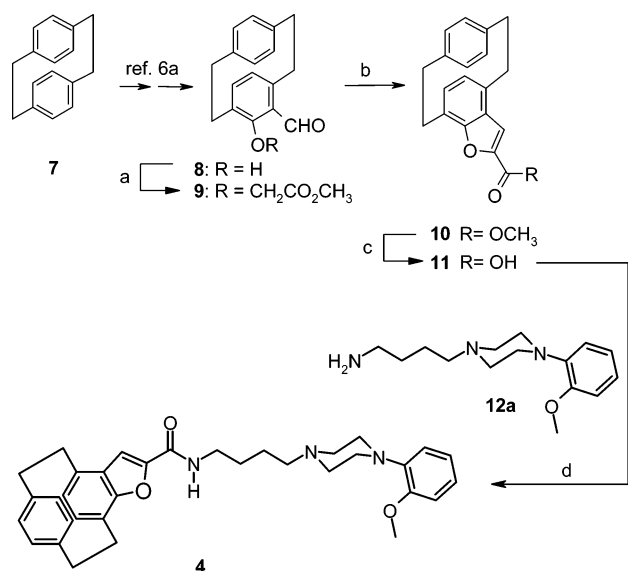
For the synthesis of target compound **4** (Scheme 1), we started from commercially available [2.2]paracyclophane (**7**). Following a five step procedure,^{6a} we obtained the double-layered salicylic aldehyde **8**, which was deprotonated with NaH and alkylated with bromoacetic acid methyl ester to give carboxylate **9** in 87% yield. Subsequent treatment with KH caused an intramolecular attack and subsequent condensation. Saponification of furanoparacyclophane **10** thus formed yielded carboxylic acid **11**, which could be activated by HATU in the presence of HOAt and, subsequently, coupled to primary amine **12a** to furnish target compound **4**.

To investigate double-layered analogues of carbocyclic D3 ligands,⁷ [2.2]paracyclophanyl carboxylic acid should be exploited as a further building block. In detail, HATU- or TBTU-supported coupling of scaffold **15**^{6b} with 2-methoxyphenylpiperazinyl-substituted butylamine **12a** and its 2,3-dichlorophenyl analogue **12b**, being readily prepared following previously described protocols,⁴ gave a 94% yield of paracyclophanyl carboxamides **6a** and **6b**, respectively (Scheme 2). Structural hybrid **12c** and 2,3-difluoro analogue **12d** were prepared employing a Buchwald–Hartwig cross-coupling reaction,^{5,8,9} which was followed by N-alkylation with 4-bromobutyronitrile and LiAlH₄-promoted reduction. Subsequent coupling with the planar-chiral building block **15**, preactivated by TBTU, yielded in bilayered carboxamides **6c** and **6d**, respectively.

Stereochemical information plays an important role in receptor recognition processes. Thus, there is continuing interest in the development of drugs as single enantiomers. Because a first screening of the cyclophane derivatives identified the racemate (*R,S*)-**6a** as a strong-binding test compound at the dopamine D3 receptor, we decided to establish the chiroselective synthesis of both enantiomers. Starting from racemic carboxylic acid **15**, pure enantiomers were obtained by resolution via the corre-

* To whom correspondence should be addressed. Tel: +49-(0)9131-8529383. Fax: +49-(0)9131-8522585. E-mail: gmeiner@pharmazie.uni-erlangen.de.

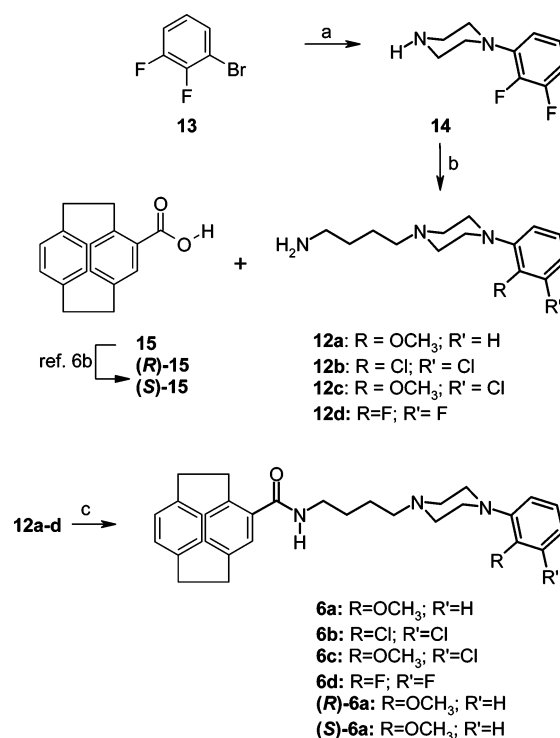
Chart 1

Scheme 1^a

^a Reagents and conditions: (a) NaH, BrCH₂CO₂CH₃, DMF, 0 °C to rt, 2 h (87%); (b) KH, NMP, 0 °C to rt, 1 h (59%); (c) 2n NaOH, MeOH, THF, 0 °C to rt, 4 h (80%) (d) HATU, HOAt, DIPEA, DMF, **12a**, CH₂Cl₂, 0 °C to rt, 1 h (81%).

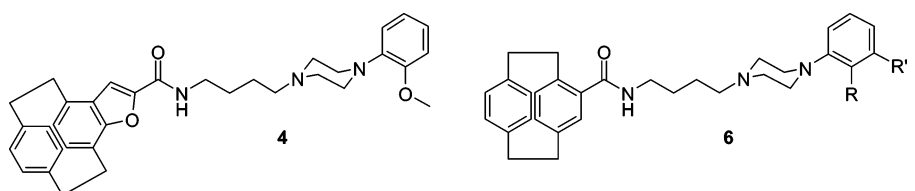
sponding diastereomeric α -(*p*-nitrophenyl)ethylammonium salts.^{6b} Subsequent activation of the enantiopure building blocks (**R**)-**15** and (**S**)-**15** by TBTU and coupling with primary amine **12a** gave access to the planar chiral enantiomers (**R**)-**6a** and (**S**)-**6a** in 85 and 86% yield, respectively.

Receptor binding experiments were established to evaluate the binding properties of target compounds **4**, (**R**)-**6a**, (**S**)-**6a**, and **6b–d** in comparison to reference agent **3a**,^{10a} a D₃ partial agonist known for highly interesting anti-dyskinetic properties and beneficial effects on cocaine-seeking behavior^{10b} (Table 1). D₁ receptor affinities were determined by utilizing porcine striatal membranes, and the D₁ selective radioligand [³H]SCH 23390.^{2a} D₂long, D₂short, D₃, and D₄ receptor affinities were

Scheme 2^a

^a Reagents and conditions: (a) Pd₂(dba)₃, BINAP, NaOt-Bu, toluene, piperazine, **13**, 115 °C, 18 h (55%); (b) 1. Br(CH₂)₃CN, K₂CO₃, MeCN, reflux, 15 h (77%); 2. LiAlH₄, Et₂O, 0 °C to rt, 1 h (88%); (c) for **6a** and **b**: HATU, DIPEA, NMP, **12a** and **b** 0 °C to rt, 1–2 h (94%); for **6c** and **d**: TBTU, DIPEA, DMF, CH₂Cl₂, **12c** and **d**, CH₂Cl₂, 0 °C to rt, 1–2 h (64–91%).

investigated by employing the cloned human dopamine receptor subtypes D₂long, D₂short,¹¹ D₃,¹² and D₄,¹³ stably expressed in Chinese hamster ovary cells (CHO) and radioligand [³H]-spiperone.^{2a} The competition data were analyzed according to a sigmoid model by nonlinear regression. Because of the observation that lead compound **3a** reveals serotonergic and

Table 1. Receptor Binding Data of **4** and **6a–d** Compared to Those of Reference Compound **3a** Utilizing Human D2_{long}, D2_{short}, D3, and D4.4 Receptors and Porcine D1, 5-HT_{1A}, 5-HT₂, and α_1 Receptors


compd	K_i (nM) ^a									
	R	R'	[³ H]SCH 23390	[³ H]spiperone				[³ H]8-OH-DPAT	[³ H]ketan-serin	[³ H]prazosin
			D1	D2 _{long}	D2 _{short}	D3	D4.4	5-HT _{1A}	5-HT ₂	α_1
4			780 ± 5.0	170 ± 30	84 ± 2.5	16 ± 1.6	140 ± 15	190 ± 38	2700 ± 300	8.4 ± 2.6
(S)- 6a	OMe	H	660 ± 30	15 ± 0.50	13 ± 1.5	3.0 ± 0.69	9.50 ± 1.5	25 ± 5.5	2300 ± 400	3.9 ± 0.20
(R)- 6a	OMe	H	490 ± 35	11 ± 2.1	5.6 ± 0.15	0.19 ± 0.009	5.40 ± 0.15	58 ± 5.5	1600 ± 250	2.5 ± 0.0
6b	Cl	Cl	2800 ± 300	220 ± 45	140 ± 35	3.6 ± 2.3	120 ± 24	660 ± 90	3500 ± 500	480 ± 80
6c	OMe	Cl	970 ± 140	42 ± 5.8	28 ± 3.4	0.46 ± 0.089	33 ± 9.5	22 ± 5.0	470 ± 95	80 ± 2.0
6d	F	F	570 ± 25	120 ± 15	35 ± 3.5	1.9 ± 0.050	18 ± 0.0	290 ± 30	1200 ± 380	45 ± 2.0
3a			760 ± 60	220 ± 19	200 ± 5.0	1.3 ± 0.096	44 ± 7.6	81 ± 8.0	840 ± 120	5.0 ± 0.40

^a K_i values in nM ± SEM are based on the means of 2–10 experiments, each done in triplicate.

adrenergic activities as well,^{10a} the test compounds were also investigated for their potency to displace [³H]8-OH-DPAT, [³H]-ketanserin, and [³H]prazosin, when employing porcine 5-HT_{1A}, 5-HT₂, and α_1 receptors, respectively.

The data from the radioligand binding studies unambiguously proved that the double-layered cyclophane-derived moiety of the target compounds is specifically recognized by the binding sites of the investigated GPCRs (Table 1). Whereas only weak to moderate binding affinities were determined for D1, 5-HT₂, and 5-HT_{1A}, D2, D4, and α_1 receptor recognition resulted in K_i values reaching even the single-digit nanomolar range. Except for furanocyclophane **4** displaying preferential α_1 binding (K_i = 8.4 nM), all test compounds preferentially associated to the dopamine D3 receptor subtype.

Because our initial screening data for paracyclophane **6a** in racemic form indicated extraordinarily high D3 binding compared to that of heterocyclic analogue **4** (K_i = 16 nM), we synthesized the pure enantiomers and subjected (**R**)-**6a** and (**S**)-**6a** to heterologous displacement experiments. In fact, we determined a K_i value of 0.19 nM for (**R**)-**6a** (FAUC 418), indicating almost 100-fold improvement compared to that of **4**, bearing the bilayered unit that is more remote from the carboxamide function. Interestingly, the structural difference being caused by the planar chirality led to a eudysmic ratio of more than 15 (K_i = 3.0 for (**S**)-**6a**). However, the 5-HT_{1A} component of (**S**)-**6a** (K_i = 25 nM) was superior compared to that of (**R**)-**6a** (K_i = 58 nM). To investigate the sensitivity of the binding profiles toward the substitution pattern of the phenyl substituent, the 2,3-dichloro, 3-chloro-2-methoxy, and 2,3-difluoro analogues **6b**, **6c**, and **6d**, respectively, were tested. In contrast to our recent observations with lead compounds of type **3** and **5**, D3 receptor binding considerably decreased for all GPCRs in this study when the 2-methoxy group was displaced (K_i = 3.6 and 1.9 nM for **6b** and **6d**, respectively). An interesting binding pattern was observed for structural hybrid **6c** with an ortho positioned methoxy group and a chloro atom in meta position displaying both high D3 affinity (K_i = 0.46 nM) and considerable selectivity over the potential anti-target α_1 (K_i = 80 nM).

As a measure of functional activity, the intrinsic activities of the paracyclophanyl carboxamides **6a–d** were determined by a mitogenesis assay measuring the rate of [³H]thymidine incorporation into growing CHO dhfr⁻ cells stably expressing the

Table 2. Intrinsic Activities Derived from the Stimulating Effect on Mitogenesis of D3 Receptor Expressing Cells and Calculated Physicochemical Properties of **4**, **6a–d** and Reference Compounds Quinpirole, **3a**, and **5**

compd	[³ H]thymidine uptake (mitogenesis) ^a			calcd physicochemical properties ^b	
	agonist effect ^c	EC ₅₀ (nM) ^d	k_B (nM) ^e	MW	clogP
4	n.d. ^f	n.d.	n.d.	637.7	6.21
6a	0%		8.5	497.7	5.65
(S)- 6a	0%		75	497.7	5.65
(R)- 6a	0%		4.7	497.7	5.65
6b	0%		110	497.7	5.65
6c	0%		18	536.5	7.17
6d	0%		10	532.1	6.28
3a	56%	1.8	n.d.	503.6	6.08
5	38%	2.0	n.d.	n.d.	n.d.
quinpirole	100%	2.6	n.d.	n.d.	n.d.

^a The values have been determined with CHO dhfr⁻ mutant cells stably expressing the human D3 receptor in 4–10 independent experiments carried out in hexaduplicates. ^b The clogP and MW values were calculated with ChemDraw Ultra 6. ^c The rate of incorporation of [³H]thymidine as evidence for mitogenesis activity relative to the maximal effect of the full agonist quinpirole (=100%) is used as a derived reference. ^d The EC₅₀ values are derived from a mean curve of three or four independent experiments. ^e The dose-dependent inhibition of the intrinsic activity of 5 nM quinpirole (inducing a 65% max. effect) derived from six to eight independent experiments, each carried out in hexaduplicates. ^f n.d. means not determined.

human D3 receptor.^{12,14,15} Although the metallocenes of type **5** (38%, EC₅₀ = 2.0 nM) could mimic the partial agonist activities of **3a** (56%, EC₅₀ = 1.8 nM),⁵ paracyclophane derivatives **6a–d** revealed an approximately neutral antagonism at the D3 receptor. The data listed in Table 2 displays k_B values between 4.7 and 110 nM indicating good correlation to the D3 binding data when the (**R**)-enantiomer of planar-chiral paracyclophane **6a** again displayed higher biological activity than the (**S**)-isomer. This finding is surprising and complementary to our previous work, where we observed partial agonist properties for all metallocenes of type **5**, whereas the intrinsic activity of the monolayered dopaminergics of type **3** strongly depended on the nature of both the heterocyclic system and the phenyl substituents giving rise to both neutral antagonists and partial agonists.

Because of the finding that not only metallocenes **5** but also sterically demanding paracyclophane derivatives can provide efficient binding to the D3 dopamine receptor subtype, we tried

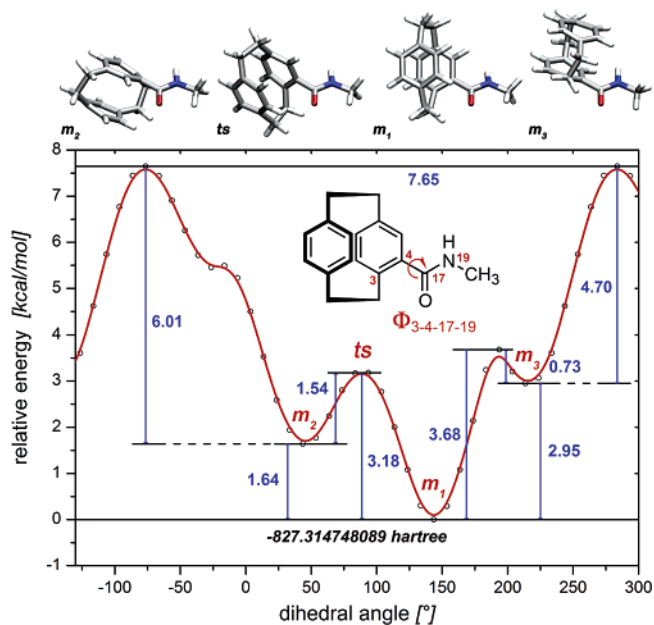


Figure 1. DFT grid-calculation of the rotational barriers and minima of the *N*-methylcarboxamide fragment of paracyclophanes **6a–d** with B3LYP/6-31G(d). For better readability, the relative energies in kcal/mol applied to the lowest energy calculated (-827.314748089 hartree) are denoted. Structures shown with the identified minima, m_1 – m_3 , and the transition state *ts* between m_1 and m_2 .

to characterize the conformational properties by employing DFT-based quantum chemical calculations on the methyl-paracyclophanylcarboxamide fragment of **6**. We further evaluated the resulting preferential structures for the conformity of their calculated magnetic shielding versus experimental NMR data. Initially, we performed a semiempirical AM1 optimization with VAMP¹⁶ on the fragment, followed by two steps of DFT calculations in Gaussian98.¹⁷ We used a B3LYP density functional with a 3-21G basis set to produce a reasonable geometry in an appropriate time. Then, we increased the basis set to the double-valence level 6-31G(d) to enhance the quality of the structure. At the same level, we accomplished a grid calculation varying the dihedral angle $\Phi_{3-4-17-19}$ in steps of 10° . With this dihedral being frozen, the rest of the system was allowed to freely adapt to the new geometry by the minimization of energy. As depicted in Figure 1, we obtained three local minima (called m_1 , m_2 , and m_3), one with the carbonyl pointing toward the proximate ethano-bridge (m_1 , $\Phi_{3-4-17-18} \approx 143.6^\circ$), the second directing the carbonyl to the interior of the bilayer (m_2 , $\Phi_{3-4-17-18} \approx 43.6^\circ$), and the third orienting its *N*–H bond toward the interior of the bilayer (m_3 , $\Phi_{3-4-17-18} \approx 213.6^\circ$). On this level of calculation, the lowest relative energy was found for m_1 , whereas m_2 and m_3 exceeded the energy of m_1 by 1.64 and 2.95 kcal/mol, respectively. The minima m_2 and m_3 are separated by a large rotational barrier of 4.70 and 6.01 kcal/mol for m_3 and m_2 , respectively. The height of this barrier can be explained not only by the fact that the orientation of the carboxamide is approximately perpendicular to the plane of the aromatic system, thus, minimizing the overlap of the π -systems, but also by the fact that the hydrogen of the amide closely approaches a hydrogen in the second aromatic layer (~ 1.9 Å). (For an extension of the discussion of rotational barriers and the characterization of the transition state *ts*, please see the Supporting Information.)

Subsequently, we subjected all three preferential conformers (m_1 , m_2 , and m_3) to a series of higher-level calculations (Table S1, Supporting Information), a method we have already applied

successfully to confirm a dominant conformer in similar studies.^{18,19} These calculations were found to give a highly consistent ranking of the conformers with almost identical relative energy differences. The energy gaps between m_1 and m_2 as well as between m_1 and m_3 only marginally decreased to 1.25 and 2.51 kcal/mol, respectively, at the highest calculation level (B3PW91/6-311+G(2df,2p)). Thus, the order of the energy content of all three conformations is retained during all calculations. According to the Boltzmann equation, the ratio of structures in the m_3 versus m_1 conformation at room temperature (298.15 K) is only about 1.44%, whereas the m_2/m_1 ratio of 12.11% indicates a putative relevance of both conformations for its biological activity. An evaluation of the energy of the transition state (*ts*) confirms that at room temperature a moderate probability exists for the transition between m_1 and m_2 .

To evaluate the relevance of the preferential structures resulting from DFT calculations and to gain further evidence for the putative bioactive conformations, we envisioned a comparison of calculated magnetic shielding with experimental NMR data. Therefore, we calculated the magnetic shielding tensor using gauge invariant atomic orbitals²⁰ (GIAO) within B3PW91/6-311+G(2d,p) or B3PW91/6-311+G(2df,2p) single-point calculations. The different orientations of the carboxamide in the three investigated conformational states and, thus, their changes of the local magnetic field by state-specific proximities to certain carbon atoms were used as a criterion to compare experimental with calculated ¹³C NMR data. As described in detail in the Supporting Information, this comparison suggests a preference for the m_1 conformer, although it is possible that the m_2 conformation also plays a role at room or body temperatures.

To understand the molecular similarity of the monolayered benzofurane-2-carboxamide moiety (**A**), the ferrocene-derived (**B**), and the respective cyclophane-derived bioisosteric element (**C**), we investigated both the steric demand and the charge distribution by mapping the electrostatic potentials onto the van der Waals surfaces.²¹ In detail, the structure of the ferrocene was derived from X-ray data²² of a suitable precursor, whereas for the cyclophane, we chose the preferential m_1 conformer from our previous DFT calculations. ESP charges were obtained consistently for all three structures using the PM3(tm) Hamiltonian within the Spartan program package.²³ The distribution of charge on the molecular surfaces was visualized with MOLCAD, implemented in Sybyl 6.9.²⁴ Figure 2 clearly shows a high degree of similarity when the molecular electrostatic properties are compared. In addition to our findings for the metallocenes, this might be the structural origin for the remarkable high target binding of the double-layered bioisosteres. Nevertheless, the ability of double-layered cyclophanes **6** to specifically bind to the GPCRs investigated is surprising because the height of the cyclophane-derived π -systems is approximately doubled (6.0 Å) compared to that of the benzofurancarboxamide substructure (3.0 Å). Moreover, the volume of the aryl fragment is increased from benzofurane (86.1 Å³) to paracyclophane (162.5 Å³) by 89%, whereas the exchange to ferrocene (108.0 Å³) extends the volume only by 25%. Thus, we were able to reconfirm that the plasticity of the binding region is substantially higher than usually expected. One main structural difference between the cyclophanylcarboxamide and the ferrocenylcarboxamide or benzofurane-2-carboxamide moieties is that one side of the carbonyl function in the cyclophane-carboxamides is prohibited for hydrogen-bond interactions with the receptor by the preferred orientation of the bulky bilayer system. This difference might have relevance for the ligand's

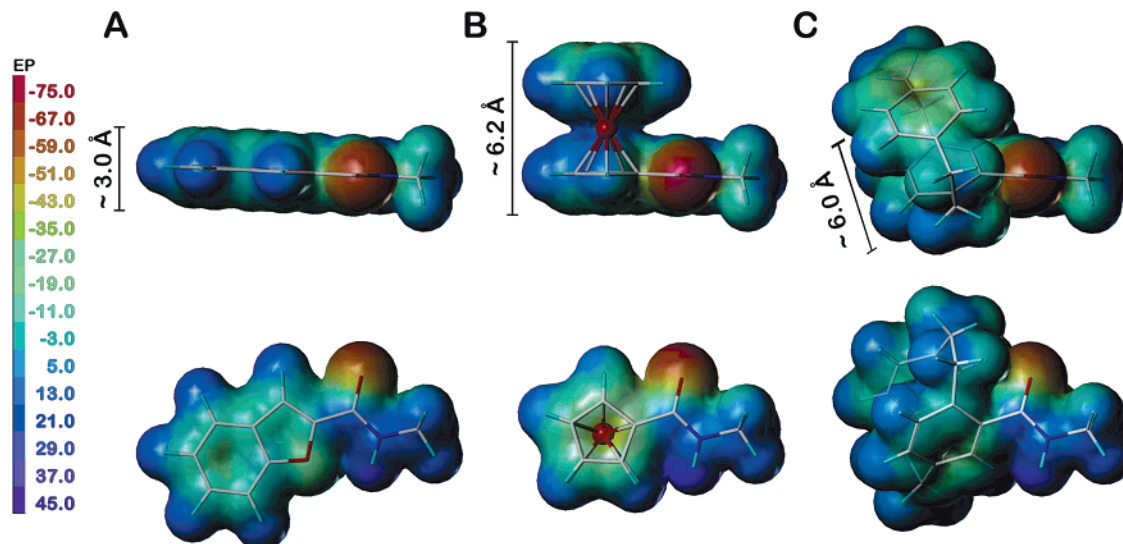


Figure 2. Electrostatic potentials mapped onto the van der Waals surfaces of *N*-methylcarboxamide fragments **A**, **B**, and **C** of monolayered benzofurane **3** and the ferrocene (**5**)- and paracyclophane (**6**)-derived bilayered bioisosteres, respectively.

inability to activate the D3 receptor observed by the absence of any intrinsic activity.

In conclusion, we have discovered novel paracyclophane-derived D3 antagonists displaying interesting binding profiles, which might be a starting point for the development of highly beneficial CNS active drugs, especially for the treatment of schizophrenia. Because of the planar chirality of the cyclophane skeleton, stereochemical differentiation was observed when the (*R*)-enantiomer (**R**)-**6a** showed significantly higher D3 affinity. Moreover, we could show that the high steric demand of the paracyclophanes of type **6** is well tolerated by the binding site of the dopamine D3 receptor, indicating substantial plasticity of the receptor-excluded volumes. Thus, the paracyclophane-derived D3 antagonists will serve as valuable molecular probes for the investigation of GPCR–ligand interactions. In contrast to our findings on the metallocenes of type **5** displaying partial agonist properties, the paracyclophanes of type **6** revealed neutral D3 antagonism.

Experimental Section

Materials and Methods. The chemicals and solvents were purchased in the highest purity available. All reactions were carried out under a nitrogen atmosphere except for ester hydrolysis. Column chromatography was performed using 60 μ m silica gel. For TLC, silica gel 60 F₂₅₄ plates were used (UV, I₂ or ninhydrin detection). Melting temperatures were uncorrected. NMR data were noted in ppm relative to TMS. IR spectroscopy was carried out on a FT/IR 410 spectrometer. MS were run on a MAT TSQ 70 spectrometer by EI (70 eV) with solid inlet. HPLC-MS were performed on an analytic HPLC system with a VWL detector, coupled to a mass spectrometer with electron spray ionization. CHN elementary analyses were performed at the Department of Organic Chemistry of the Friedrich-Alexander University.

***N*-[4-(4-(2-Methoxyphenyl)piperazin-1-yl)butyl-1(4,7)-benzofurano-4-(1,4)-benzohexaphanyl-1²-carboxamide (4).** To a solution of **11** (35.0 mg, 0.12 mmol) and DIPEA (0.05 mL, 0.24 mmol) in CH₂Cl₂ (5 mL) was added HATU (47.0 mg, 0.13 mmol) and HOAt (17.0 mg, 0.12 mmol) in DMF (2 mL) at 0 °C. After the addition of **12a** (34.0 mg, 0.13 mmol) in CH₂Cl₂ (5 mL), the mixture was stirred at 0 °C for 1 h. Then, CH₂Cl₂ and aqueous saturated NaHCO₃ were added. The organic layer was dried (MgSO₄) and evaporated, and the residue was purified by flash chromatography (CH₂Cl₂/MeOH 98:2) to give **4** (52.0 mg, 81%) as a white solid. Mp 81–82 °C. ¹H NMR (CDCl₃, 360 MHz): δ 1.69–1.82 (m, 4H), 2.57 (t, *J* = 7.4 Hz, 2H), 2.74–2.76 (m, 4H), 2.86–2.93 (m,

2H), 2.96–3.03 (m, 4H), 3.13–3.15 (m, 4H), 3.31–3.36 (m, 1H), 3.50–3.56 (m, 2H), 3.60–3.65 (m, 1H), 3.85 (s, 3H), 6.03 (dd, *J* = 1.9 Hz, *J* = 7.9 Hz, 1H), 6.13 (dd, *J* = 1.9 Hz, *J* = 7.9 Hz), 6.42 (dd, *J* = 1.8 Hz, *J* = 7.8 Hz), 6.47 (dd, *J* = 1.8 Hz, *J* = 7.8 Hz), 6.55 (d, *J* = 7.6 Hz, 1H), 6.65 (d, *J* = 7.6 Hz, 1H), 6.81 (br t, *J* = 5.5 Hz, 1H), 6.85 (dd, *J* = 1.2 Hz, *J* = 8.2 Hz, 1H), 6.83–6.95 (m, 2H), 6.99 (dd, 1.2 Hz, *J* = 8.2 Hz, 1H), 7.27 (s, 1H). ¹³C NMR (CDCl₃, 90 MHz): δ 24.2, 27.7, 29.9, 32.4, 34.2, 34.7, 39.3, 50.5, 53.5, 55.3, 58.1, 111.2, 111.4, 118.2, 120.9, 122.8, 123.3, 125.3, 128.1, 128.9, 131.1, 131.9, 132.6, 136.1, 137.9, 138.4, 141.3, 147.4, 152.3, 154.5, 159.4. EI-MS *m/z*: 537 (M⁺). Anal. (C₃₄H₃₉N₃O₃): C, H, N.

***N*-[4-[4-(2-Methoxyphenyl)piperazin-1-yl]butyl][2.2]-paracyclophane-4-carboxamide (6a).** To a solution of racemic **15**²⁵ (synth. according to literature^{6b}) (30.0 mg, 0.12 mmol) and DIPEA (0.05 mL, 0.24 mmol) in CH₂Cl₂ (4 mL) was added HATU (47.0 mg, 0.12 mmol) in NMP (2 mL) at 0 °C. After the addition of **12a** (34.0 mg, 0.13 mmol), the mixture was stirred at room temperature for 0.5 h. Then, CH₂Cl₂ and aqueous saturated NaHCO₃ were added. The organic layer was dried (MgSO₄) and evaporated, and the residue was purified by flash chromatography (CH₂Cl₂/MeOH 98:2) to give pure **6a** (56 mg, 94%) as a colorless oil. ¹H NMR (CDCl₃, 600 MHz): δ 1.69–1.87 (m, 4H), 2.82–3.23 (m, 17H), 3.41–3.50 (m, 2H), 3.60–3.69 (m, 1H), 3.84 (s, 3H), 6.32 (br t, *J* = 5.9 Hz, 1H), 6.44–6.50 (m, 3H), 6.54 (s, 1H), 6.57 (dd, *J* = 7.9 Hz, *J* = 1.8 Hz, 1H), 6.68–6.73 (m, 2H), 6.81–6.93 (m, 3H), 6.97–7.01 (m, 1H). ¹³C NMR (CDCl₃, 90 MHz): δ 24.4, 27.5, 34.7, 35.1, 35.3, 35.4, 39.6, 50.3, 53.3, 55.3, 57.9, 111.2, 118.2, 120.9, 122.9, 131.7, 132.0, 132.4, 132.5, 132.6, 134.8, 135.2, 135.8, 138.9, 139.1, 139.8, 140.1, 141.2, 152.2, 169.4. EI-MS *m/z*: 498 (M⁺). Anal. (C₃₂H₃₉N₃O₂ + 0.3 H₂O): C, H, N.

***N*-[4-(4-(2,3-Dichlorophenyl)piperazin-1-yl)butyl][2.2]-paracyclophane-4-carboxamide (6b).** Compound **13**²⁵ (30.0 mg, 0.12 mmol), DIPEA (0.05 mL, 0.24 mmol), HATU (47.0 mg, 0.13 mmol), and **12b** (0.04 g, 0.13 mmol) were reacted and worked up as described for **6a** to give **6b** (60.0 mg, 94%) as a colorless oil. ¹H NMR (CDCl₃, 360 MHz): δ 1.60–1.69 (m, 4H), 2.44 (t, *J* = 6.6 Hz, 2H), 2.55–2.57 (m, 4H), 2.88–3.20 (m, 8H), 3.41–3.47 (m, 2H), 3.62–3.69 (m, 1H), 6.28 (br t, *J* = 5.5 Hz, 1H), 6.42 (d, *J* = 7.8 Hz, 1H), 6.45 (d, *J* = 7.8 Hz, 1H), 6.53–6.57 (m, 3H), 6.65 (d, *J* = 2.0 Hz, 1H), 6.84–6.88 (m, 2H), 7.09–7.16 (m, 2H). ¹³C NMR (CDCl₃, 90 MHz): δ 24.5, 27.6, 34.7, 35.1, 35.3, 35.4, 39.7, 51.0, 53.2, 57.9, 118.6, 124.5, 127.3, 127.5, 131.7, 132.0, 132.5, 132.6, 134.8, 133.9, 135.2, 135.8, 138.9, 139.1, 139.8, 140.1, 151.1, 169.4. EI-MS *m/z*: 535, 537 (M⁺). Anal. (C₃₁H₃₅Cl₂N₃O): C, H, N.

N-4-[4-(3-Chloro-2-methoxyphenyl)piperazin-1-yl]butyl][2.2]-paracyclophane-4-carboxamide (6c). To a solution of **15**²⁵ (30.0 mg, 0.12 mmol) and DIPEA (0.07 mL, 0.42 mmol) in CH₂Cl₂ (4 mL) was added TBTU (42.0 mg, 0.13 mmol) in DMF (0.30 mL) at 0 °C. After the addition of **12c** (39.0 mg, 0.13 mmol) in CH₂Cl₂ (5 mL), the mixture was stirred for 30 min at room temperature. Then, CH₂Cl₂ and aqueous saturated NaHCO₃ were added. The organic layer was dried (MgSO₄) and evaporated, and the residue was purified by flash chromatography (CH₂Cl₂/MeOH 98:2) to give pure **6c** (58.0 mg, 91%) as a colorless oil. ¹H NMR (CDCl₃, 360 MHz): δ 1.61–1.69 (m, 4H), 2.43 (t, *J* = 6.7 Hz, 2H), 2.54–2.56 (m, 4H), 2.82–3.00 (m, 8H), 3.42–3.47 (m, 2H), 3.62–3.69 (m, 1H), 6.23 (br t, *J* = 3.4 Hz, 1H), 6.41 (d, *J* = 7.8 Hz, 1H), 6.45 (d, *J* = 7.8 Hz, 1H), 6.54–6.57 (m, 3H), 6.64 (d, *J* = 2.1 Hz, 1H), 6.71 (d, *J* = 1.6 Hz, d, *J* = 8.1 Hz, 2H), 6.99 (d, *J* = 1.6 Hz, d, *J* = 8.1 Hz, 2H). ¹³C NMR (CDCl₃, 90 MHz): δ 24.5, 27.5, 34.7, 35.1, 35.3, 35.4, 39.6, 49.9, 53.6, 57.9, 58.9, 117.1, 123.2, 124.5, 128.7, 131.7, 132.0, 132.4, 132.5, 132.6, 134.9, 135.2, 135.8, 138.9, 139.1, 139.8, 140.1, 146.5, 148.6, 169.4. EI-MS *m/z*: 531, 533 (M⁺). Anal. (C₃₂H₃₈ClN₃O₂ · 0.33 H₂O): C, H, N.

N-[4-[4-(2,3-Difluorophenyl)piperazin-1-yl]butyl][2.2]-paracyclophane-4-carboxamide (6d). To a solution of **15**²⁵ (30.0 mg, 0.12 mmol) and DIPEA (0.07 mL, 0.42 mmol) in CH₂Cl₂ (4 mL) was added TBTU (42.0 mg, 0.13 mmol) in DMF (0.30 mL) at 0 °C. After the addition of **12d** (36.0 mg, 0.13 mmol) in CH₂Cl₂ (5 mL), the mixture was stirred at room temperature for 1 h. Then, CH₂Cl₂ and aqueous saturated NaHCO₃ were added. The organic layer was dried (MgSO₄) and evaporated, and the residue was purified by flash chromatography (CH₂Cl₂/MeOH 98:2) to give **6d** (38.0 mg, 64%) as a colorless oil. ¹H NMR (CDCl₃, 360 MHz): δ 1.61–1.69 (m, 4H), 2.44 (t, *J* = 6 Hz, 2H), 2.55–2.57 (m, 4H), 2.84–3.30 (m, 8H), 3.41–3.47 (m, 2H), 3.65 (ddd, *J* = 2.5 Hz, *J* = 10.2 Hz, *J* = 12.7 Hz, 1H), 6.17 (br t, *J* = 6.1 Hz, 1H), 6.41 (d, *J* = 7.8 Hz, 1H), 6.45 (d, *J* = 7.8 Hz, 1H), 6.53–6.60 (m, 4H), 6.65 (d, *J* = 1.8 Hz, 1H), 6.71–6.79 (m, 1H), 6.84 (d, *J* = 7.3 Hz, 1H), 6.90–6.97 (m, 1H). ¹³C NMR (CDCl₃, 90 MHz): δ 24.4, 27.6, 34.7, 35.1, 35.3, 35.4, 39.7, 50.2, 53.1, 57.9, 109.9 (d, *J* = 8.0 Hz), 113.6–113.7 (m, 1C), 123.5 (dd, *J* = 2.8 Hz, *J* = 5.5 Hz, 1C), 131.6, 132.0, 132.4, 132.5, 132.6, 134.8 (C-7), 135.2, 135.8, 141.9 (dd, *J* = 2.8 Hz, *J* = 5.5 Hz), 143.5 (d, *J* = 8.0 Hz, *J* = 247.3 Hz), 151.5 (dd, *J* = 8.0 Hz, *J* = 247.3 Hz), 169.4 (CO). EI-MS *m/z*: 503 (M⁺). Anal. (C₃₁H₃₅F₂N₃O 0.25 H₂O): C, H, N.

(S)-N-[4-[4-(2-Methoxyphenyl)piperazin-1-yl]butyl][2.2]-paracyclophane-4-carboxamide (S)-(6a). Compound **(S)-15**^{6b} (30.0 mg, 0.12 mmol), DIPEA (0.05 mL, 0.24 mmol), HATU (47.0 mg, 0.13 mmol), and **12a** (34.0 mg, 0.13 mmol) were reacted and worked up as described for **6a** to give **(S)-6a** (51.0 mg, 85%) as a colorless oil. [α]_D²⁵ + 65 °C (c 0.5, CHCl₃). ¹H NMR (CDCl₃, 360 MHz): 1.64–1.70 (m, 4H), 2.49 (t, *J* = 7.0 Hz, 2H), 2.64–2.66 (m, 4H), 2.87 (ddd, *J* = 5.5 Hz, *J* = 10.2 Hz, 12.7 Hz, 1H), 2.94–2.97 (m, 1H), 2.97–3.03 (m, 4H), 3.07 (ddd, *J* = 2.5 Hz, *J* = 10.2 Hz, *J* = 12.7 Hz, 1H), 3.11–3.17 (m, 2H), 3.25 (ddd, *J* = 5.5 Hz, *J* = 10.2 Hz, *J* = 12.7 Hz), 3.42–3.46 (m, 2H), 3.66 (ddd, *J* = 2.5 Hz, *J* = 10.2 Hz, *J* = 12.7 Hz, 1H), 3.84 (s, 3H), 6.23 (br t, *J* = 5.5 Hz, 1H), 6.41–6.42 (m, 1H), 6.46 (d, *J* = 8.0 Hz, 1H), 6.53 (m, 2H), 6.56 (dd, *J* = 1.8 Hz, *J* = 8.0 Hz), 6.66 (d, *J* = 1.8 Hz, 1H), 6.81 (m, 1H), 6.845 (dd, *J* = 1.2 Hz, *J* = 8.5 Hz, 1H), 6.85 (dd, *J* = 1.5 Hz, *J* = 7.8 Hz, 1H), 6.90 (ddd, *J* = 1.2 Hz, *J* = 7.8 Hz, *J* = 7.8 Hz), 6.99 (ddd, *J* = 1.5 Hz, *J* = 7.5 Hz, 7.5 Hz, 1H). ¹³C NMR (CDCl₃, 90 MHz): δ (ppm): 24.3, 27.5, 34.8, 35.1, 35.3, 35.5, 39.6, 50.2, 53.4, 55.4, 57.9, 111.2, 118.3, 120.9, 123.0, 131.5, 132.1, 132.4, 132.5, 132.6, 134.9, 135.2, 135.9, 139.0, 139.2, 139.9, 140.1, 141.1, 152.3, 169.4. IR (NaCl): 3316, 2930, 2812, 1638 cm⁻¹. APCI-MS *m/z*: 498 ((M + H)⁺). Anal. (C₃₂H₃₉N₃O₂ 0.6 H₂O): C, H, N.

(R)-N-[4-[4-(2-Methoxyphenyl)piperazin-1-yl]butyl][2.2]-paracyclophane-4-carboxamide (R)-(6a). Compound **(R)-15**^{6b} (30.0 mg, 0.12 mmol), DIPEA (0.05 mL, 0.24 mmol), HATU (47.0 mg, 0.13 mmol), and **12a** (34.0 mg, 0.13 mmol) were reacted and worked up as described for **6a** to give **(R)-6a** (53.0 mg, 88%) as a colorless oil. [α]_D²⁵ -70 °C (c 0.5, CHCl₃). IR (NaCl): 3316, 2930,

2812, 1638 cm⁻¹. APCI-MS *m/z*: 498 ((M + H)⁺). Anal. (C₃₂H₃₉N₃O₂ 0.3 H₂O): C, H, N.

[2.2]Paracyclophane-4-carboxylic Acid (15) Compound **15**²⁵ was synthesized according to literature.^{6b} To a stirred solution of 4-bromo[2.2]paracyclophane²⁶ (2.08 g, 7.25 mmol) in dry Et₂O (135 mL), *n*-butyllithium (4.50 mL of a 2.5 M solution in hexane, 11.20 mmol) was added dropwise under nitrogen. Then, the mixture was stirred at room temperature for 2 h. Then, an excess of dried dry ice was added. The reaction was allowed to warm to room temperature, the solvent was evaporated to dryness, and the solid residue was dissolved in H₂O (200 mL). Insoluble [2.2]paracyclophane was filtered off, and the aqueous phase was thoroughly washed with ether and CH₂Cl₂ to remove traces of the added CH₂Cl₂, and the mixture was extracted with CH₂Cl₂. The aqueous layers were combined and acidified with concentrated hydrochloric acid to pH 3 and extracted with CHCl₃. The combined organic layer was dried (MgSO₄) and evaporated to give [2.2]paracyclophanyl-4-carboxylic acid (1.25 g, 61%) as a white solid. Mp 223–224 °C (ref 25 mp 223.5–224.5 °C).

(S)-[2.2]Paracyclophane-4-carboxylic Acid (S)-15. The resolution of **15**²⁵ was accomplished according to ref 6b^{6b} to give 0.30 g (63%) of (S)-(+)-[2.2]paracyclophane-4-carboxylic acid. [α]_D²⁵ +172 (c 0.5 CHCl₃), (ref 27 [α]_D²⁵ +164).

(R)-[2.2]Paracyclophane-4-carboxylic Acid (R)-15. The resolution of **15**²⁵ was accomplished according to ref 6b to give 5.00 mg (20%) of (R)-(–)-[2.2]paracyclophane-4-carboxylic acid. [α]_D²⁵ -164.5 (c 0.5 CHCl₃), (ref 25 [α]_D²⁵ -157).

(4-Formyl[2.2]paracyclophane-5-yloxy)acetic Acid Methyl Ester (9). To a solution of 4-formyl-5-hydroxy[2.2]paracyclophane **8** (synthesized according to ref 6a) (70.0 mg, 0.28 mmol) in dry DMF (5 mL) was added dropwise a suspension (3 mL) of NaH (40.0 mg) in DMF (9 mL) at 0 °C. Then, the reaction mixture was allowed to warm to room temperature and stirred for 1 h at room temperature. The mixture was extracted with aqueous saturated NaHCO₃ and Et₂O. After washing with citronic acid (5%), aqueous saturated NaCl, and water, the combined organic layers were dried (MgSO₄) and evaporated, and the residue was purified by flash chromatography (hexanes/EtOAc 9:1) to give (4-formyl[2.2]paracyclophane-5-yloxy)acetic acid methyl ester (**9**) (78.0 mg, 87%) as a white solid. Mp 97–99 °C. ¹H NMR (CDCl₃, 360 MHz): δ 2.72–2.85 (m, 3H), 2.99–3.31 (m, 9H), 3.75 (s, 3H), 4.03–4.11 (m, 1H), 4.43 (d, *J* = 15.6 Hz, 1H), 4.72 (d, *J* = 15.6 Hz, 1H), 6.40 (dd, *J* = 1.8 Hz, *J* = 7.8 Hz, 1H), 6.44 (d, *J* = 7.8 Hz, 1H), 6.45 (d, *J* = 7.8 Hz, 1H), 6.59 (dd, *J* = 1.8 Hz, *J* = 7.8 Hz, 1H), 6.67 (d, *J* = 7.8 Hz, 1H), 6.84 (dd, *J* = 1.8 Hz, *J* = 7.8 Hz, 1H), 10.36 (s, 1H). ¹³C NMR (CDCl₃, 90 MHz): δ 31.5, 33.8, 34.1, 34.2, 52.1, 71.4, 129.4, 130.0, 130.9, 131.4, 131.7, 132.0, 132.4, 133.2, 133.4, 139.1, 140.8, 144.4, 161.6, 169.2, 192.8. EI-MS *m/z*: 324 (M⁺).

1(4,7)Benzofurano-4(1,4)benzenehexaphanyl-1²-carboxylic Acid Methyl Ester (10). To a solution of (4-formyl[2.2]paracyclophane-5-yloxy)acetic acid methyl ester (**9**) (0.13 g, 0.40 mmol) in dry NMP (10 mL) was added dropwise a suspension (5 mL, 0.44 mmol) of KH (36.0 mg) in DMF (10 mL) at 0 °C. Then, the reaction mixture was allowed to warm to room temperature and stirred for 1 h at room temperature. The mixture was extracted with aqueous saturated NaHCO₃ and Et₂O. After washing with aqueous saturated NaCl, the combined organic layers were dried (MgSO₄) and evaporated, and the residue was purified by flash chromatography (hexanes/EtOAc 9:1) to give 1(4,7)benzofurano-4(1,4)benzenehexaphanyl-1²-carboxylic acid methyl ester (**10**) (72.0 mg, 59%) as a white solid. Mp 215–217 °C. ¹H NMR (CDCl₃, 360 MHz): δ 2.83–2.96 (m, 2H), 2.97–3.13 (m, 4H), 3.30–3.34 (m, 1H), 3.64 (m, 1H), 4.01 (s, 3H), 6.04 (d, *J* = 1.8 Hz, *J* = 7.8 Hz, 1H), 6.09 (d, *J* = 1.8 Hz, *J* = 7.8 Hz, 1H), 6.41 (dd, *J* = 1.8 Hz, *J* = 7.8 Hz, 1H), 6.47 (dd, *J* = 1.8 Hz, *J* = 7.8 Hz, 1H), 6.56 (d, *J* = 7.5 Hz, 1H), 6.68 (d, *J* = 7.5 Hz, 1H), 7.31 (s, 1H). ¹³C NMR (CDCl₃, 90 MHz): δ 34.9, 35.1, 35.3, 36.2, 51.6, 112.8, 129.6, 131.8, 132.3, 132.8, 133.1, 136.2, 136.4, 137.4, 139.4, 140.0, 140.1, 143.8, 172.0. EI-MS *m/z*: 306 (M⁺).

1-(4,7) Benzofurano-4-(1,4)benzene-hexaphanyl-1²-carboxylic Acid (11). To a solution of 1(4,7)benzofurano-4(1,4)benzene-hexaphanyl-1²-carboxylic acid methyl ester (**10**) (11.0 mg, 0.04 mmol) in THF (1 mL), MeOH (1 mL) and aqueous NaOH (2N, 0.50 mL) were added at 0 °C. The mixture was stirred at room temperature for 4 h and left for 1 h under ultra sonic assistance. After evaporation in vacuo (40 °C, 100 mbar), the residue was diluted with water and washed with Et₂O. After acidification with HCl (2 N) to pH 2 and extraction with Et₂O, the organic layer was dried (MgSO₄) and evaporated, and the residue was purified by flash chromatography (CH₂Cl₂/MeOH 98:2) to give **11** (9.0 mg, 80%) as a white solid. Mp 234–236 °C. ¹H NMR (CDCl₃, 360 MHz): δ 2.87–2.96 (m, 2H), 2.98–3.16 (m, 4H), 3.34–3.71 (m, 2H), 4.77 (br s., 1H), 6.08 (d, *J* = 1.8 Hz, *J* = 7.8 Hz, 1H), 6.15 (d, *J* = 1.8 Hz, *J* = 7.8 Hz, 1H), 6.43 (dd, *J* = 1.8 Hz, *J* = 7.8 Hz), 6.49 (dd, *J* = 1.8 Hz, *J* = 7.8 Hz), 6.61 (d, *J* = 7.5 Hz, 1H), 6.73 (d, *J* = 7.5 Hz, 1H), 7.48 (s, 1H). ¹³C NMR (CDCl₃, 90 MHz): δ 29.7, 31.7, 33.6, 34.2, 114.7, 123.7, 124.9, 127.6, 128.8, 130.6, 131.8, 132.4, 133.2, 136.5, 137.7, 138.6, 155.7, 161.8. EI-MS *m/z*: 292 (M⁺). Anal. (C₁₉H₁₆O₃ · 0.11 H₂O): C, H, N.

4-[4-(2,3-Difluorophenyl)piperazin-1-yl]butylamine (12d). To a solution of piperazine (1.12 g, 13.0 mmol), NaO^tBu (0.68 g, 7.0 mmol), Pd₂(dba)₃ (0.05 g, 0.50 mol %), BINAP (2,2'-bis(diphenylphosphino)-1,1'-binaphthalin (0.09 g, 2.00 mol %) in toluene (20 mL) was added 1-bromo-2,3-difluorobenzene (**13**) (0.56 mL, 5.00 mmol). The reaction mixture was heated for 18 h to 115 °C, cooled to room temperature, filtered through Celite, and evaporated, yielding **14** (0.55 g, 55%) as a yellow oil. ¹H NMR (CDCl₃, 360 MHz): δ 2.48–2.50 (m, 4H), 3.12–3.15 (m, 4H), 6.67–6.71 (m, 1H), 6.73–6.80 (m, 1H), 6.92–6.99 (m, 1H). IR (NaCl): 3421, 2925, 2852, 1620 cm⁻¹. EI-MS *m/z*: 198 (M⁺).

To a solution of **14** (0.39 g, 1.95 mmol) and Na₂CO₃ (0.50 g, 4.70 mmol) in acetonitrile (10 mL) was added bromobutyronitrile (0.15 mL, 1.55 mmol), and the mixture was refluxed for 15 h. After cooling to room temperature, the mixture was dried (MgSO₄) and evaporated, and the residue was purified by flash chromatography (CHCl₃/EtOAc 1:1) to give 4-[4-(2,3-difluorophenyl)piperazin-1-yl]butyronitrile (0.50 g, 77%) as a colorless oil. ¹H NMR (CDCl₃, 360 MHz): δ 1.83–1.90 (m, 2H), 2.46 (t, *J* = 6.9 Hz, 2H), 2.53 (t, *J* = 6.9 Hz, 2H), 2.44–2.48 (m, 4H), 2.60–2.63 (m, 4H), 6.66–6.71 (m, 1H), 6.74–6.81 (m, 1H), 6.93–6.99 (m, 1H). EI-MS *m/z*: 265 (M⁺).

To a solution of 4-[4-(2,3-difluorophenyl)piperazin-1-yl]butyronitrile (0.15 g, 0.50 mmol) in Et₂O (5 mL), LiAlH₄ (1 M in Et₂O, 1.00 mL) was added dropwise at 0 °C and stirred at room temperature for 1 h. After the addition of aqueous saturated NaHCO₃ at 0 °C, the residue was filtered (Celite/MgSO₄/Celite), washed with CH₂Cl₂, and evaporated to give **12d** (0.14 g, 95%) as a yellow oil. ¹H NMR (CDCl₃, 360 MHz): δ 1.47–1.60 (m, 4H), 2.39–2.44 (m, 2H), 2.61–2.65 (m, 4H), 2.71–2.75 (m, 2H), 3.12–3.15 (m, 4H), 6.67–6.71 (m, 1H), 6.73–6.80 (m, 1H), 6.92–6.99 (m, 1H). ¹³C NMR (CDCl₃, 90 MHz): δ 24.2, 31.5, 41.9, 45.9, 51.5, 58.4, 109.9, 113.6–113.7, 123.5, 141.9, 144.0, 151.5. EI-MS *m/z*: 269 (M⁺).

Determination of Enantiomeric Excess. Enantiomeric excess was determined by HPLC analysis using an Agilent system in combination with ChemStation software (hexane/2-propanol; isocratic 60/40), a CHIRACEL OD chiral column (0.64 × 20 cm), and a flow rate of 1 mL/min; 210 nm; *R*_t (**S**)-**6a** = 16.8 min, *R*_t (**R**)-**6a** = 21.2 min.

Receptor Binding Experiments. Receptor binding studies were carried out as described in the literature.² In brief, the dopamine D1 receptor assay was done with porcine striatal membranes at a final protein concentration of 40 μg/assay tube and the radioligand [³H]SCH 23390 at 0.3 nM (*K*_d = 0.11–0.62 nM). Competition experiments with the human D2_{long}, D2_{short}, D3, and D4.4 receptors were run with preparations of membranes from CHO cells expressing the corresponding receptor and [³H]spiperone at a final concentration of 0.1 nM. The assays were carried out with a protein concentration of 3–20 μg/assay tube and *K*_d values of 0.12–0.15 nM for D2_{long}, 0.10 nM for D2_{short}, 0.18–0.35 nM for D3, and

0.25–0.48 nM for D4.4. Unspecific binding was determined using 10 μM haloperidole.

The investigation of serotonin 5-HT_{1A} and 5-HT₂ and adrenergic α₁ binding was performed as described in literature.⁵ In brief, porcine cortical membranes were subjected to the binding assay at a concentration of 80–115 μg/assay tube for the determination of 5-HT_{1A} and 5-HT₂ binding utilizing [³H]8-OH-DPAT and [³H]-ketanserin, each at a final concentration of 0.5 nM with *K*_d values of 0.92–2.6 nM (for 5-HT_{1A}) and 1.9–2.5 nM (for 5-HT₂). Cortical membranes at 55–80 μg/assay tube and the radioligand [³H]-prazosin at a final concentration of 0.4 nM were applied to determine adrenergic α₁ binding with *K*_d values of 0.10 nM. For the investigation of unspecific binding serotonin, methysergid and prazosin were used, each at a concentration of 10 μM when measuring 5-HT_{1A}, 5-HT₂, and α₁ affinities.

Protein concentration was established by the method of Lowry using bovine serum albumin as the standard.²⁸

Data analysis of the resulting competition curves was accomplished by nonlinear regression analysis using the algorithms in PRISM (GraphPad Software, San Diego, CA). The *K*_i values were derived from the corresponding EC₅₀ data utilizing the equation of Cheng and Prusoff.²⁹

Mitogenesis Experiments. The determination of the stimulating effect of the test compounds on mitogenesis as a functional assay was done with a CHO dhfr⁻ cell line stably transfected with the human dopamine D3 receptor, according to literature.^{4a,12,14a} In detail, 10 000 cells/well were grown for 72 h in a 96-well plate in the appropriate medium supplemented with serum. After washing and adding a serum free medium, the cells were incubated for 20 h with the test compound at eight different concentrations in the range of 0.01–10 000 nM as hexaduplicates. After the addition of 0.02 μCi/well of [³H]thymidine (specific activity 25 Ci/mmol, Amersham Biosciences), incubation was continued for 4 h. Finally, the cells were harvested, and the incorporated radioactivity was measured with a microplate scintillation counter.

Experimental data resulting from the mitogenesis assay were normalized and then combined to obtain a mean curve. Nonlinear regression analysis of this curve provided the EC₅₀ value as a measure of potency. The top value of the curve represented intrinsic activity, which was correlated to the effect of the full agonist quinpirole (100%).

Computational Investigations. Molecular modeling investigations were performed on Silicon Graphics Indigo2 and Octane2 workstations. Quantum chemical calculations with a total of approximately 1700 processor hours were performed on a 4-node dual Xeon mini-cluster as well as in part on a 150-node dual Xeon cluster at the High Performance Computing division of the Friedrich-Alexander University.

Acknowledgment. We thank Dr. H. H. M. Van Tol (Clarke Institute of Psychiatry, Toronto), Dr. J. -C. Schwartz, and Dr. P. Sokoloff (INSERM, Paris) as well as J. Shine (The Garvan Institute of Medical Research, Sydney) for providing dopamine D₄, D₃, and D₂ receptor expressing cell lines, respectively. We also acknowledge Dr. G. Wellein and Dr. G. Hager (High Performance Computing division of the “Regionales Rechenzentrum Erlangen”) for their collaboration during calculations on a 150-node dual Xeon cluster. This work was supported by the BMBF and Fonds der Chemischen Industrie.

Supporting Information Available: Extended discussion about rotational barriers, calculation of magnetic shielding properties, and elemental analysis data.

References

- Chen, X.; Wang, W. The use of bioisosteric groups in lead optimization. *Annu. Rep. Med. Chem.* **2003**, *38*, 333–346.
- (a) Hübner, H.; Haubmann, C.; Utz, W.; Gmeiner, P. Conjugated enynes as nonaromatic catechol bioisosteres: synthesis, binding experiments, and computational studies of novel dopamine receptor agonists recognizing preferentially the D3 subtype. *J. Med. Chem.*

- 2000, 43, 756–762. (b) Lenz, C.; Haubmann, C.; Huebner, H.; Boeckler, F.; Gmeiner, P. Fancy bioisosteres: synthesis and dopaminergic properties of the endiyme FAUC 88 as a novel nonaromatic D3 agonist. *Bioorg. Med. Chem.* **2005**, 13, 185–191.
- (3) (a) Ortner, B.; Waibel, R.; Gmeiner, P. Indoloparacyclophanes: synthesis and dopamine receptor binding of a novel arylbioisostere. *Angew. Chem., Int. Ed.* **2001**, 40, 1283–1285. (b) Ortner, B.; Hübner, H.; Gmeiner, P. Planar chiral indoles: synthesis and biological effects of the enantiomers. *Tetrahedron: Asymmetry* **2001**, 12, 3205–3208.
- (4) (a) Bettinetti, L.; Schlotter, K.; Hübner, H.; Gmeiner, P. Interactive SAR studies: rational discovery of super-potent and highly selective dopamine D3 receptor antagonists and partial agonists. *J. Med. Chem.* **2002**, 45, 4594–4597. (b) Boeckler, F.; Leng, A.; Mura, A.; Bettinetti, L.; Feldon, J.; Gmeiner, P.; Ferger, B. Attenuation of 1-methyl-4-phenyl-1,2,3,6-tetrahydropyridine (MPTP) neurotoxicity by the novel selective dopamine D3-receptor partial agonist FAUC 329 predominantly in the nucleus accumbens of mice. *Biochem. Pharmacol.* **2003**, 66, 1025–1032.
- (5) Schlotter, K.; Boeckler, F.; Hübner, H.; Gmeiner, P. Fancy bioisosteres: metallocene-derived G-protein-coupled receptor ligands with subnanomolar binding affinity and novel selectivity profiles. *J. Med. Chem.* **2005**, 48, 3696–3699.
- (6) (a) Rozenberg, V.; Danilova, T. Y.; Sergeeva, E.; Vorontsov, E.; Starikova, Z.; et al. Resolution and novel reactions of 4-hydroxy-[2.2]paracyclophane. *Eur. J. Org. Chem.* **2002**, 468–477. (b) Rozenberg, V.; Bubrovina, N.; Sergeeva, E.; Antonov, D.; Belokon, Y. An improved synthesis of (S)-(+)- and (R)-(-)-[2.2]paracyclophane-4-carboxylic acid. *Tetrahedron: Asymmetry* **1998**, 9, 653–656.
- (7) Leopoldo, M.; Berardi, F.; Colabufo, N. A.; De Giorgio, P.; Lacivita, E.; Perrone, R.; Tortorella, V. Structure-affinity relationship study on *N*-[4-(4-arylpiperazin-1-yl)butyl]arylcaboxamides as potent and selective dopamine D3 receptor ligands. *J. Med. Chem.* **2002**, 45, 5727–5735.
- (8) (a) Wolfe, J. P.; Tomori, H.; Sadighi, J. P.; Yin, J.; Buchwald, S. L. Simple, efficient catalyst system for the palladium-catalyzed amination of aryl chlorides, bromides, and triflates. *J. Org. Chem.* **2000**, 65, 1158–1174. (b) Hartwig, J. F. Transition metal catalyzed synthesis of arylamines and aryl ethers from aryl halides and triflates: scope and mechanism. *Angew. Chem., Int. Ed.* **1998**, 37, 2046–2067.
- (9) (a) Nishiyama, M.; Yamamoto, T.; Koie, Y. Synthesis of *N*-arylpiperazines from aryl halides and piperazine under a palladium tri-*tert*-butylphosphine catalyst. *Tetrahedron Lett.* **1998**, 39, 617–620. (b) Torisawa, Y.; Nishi, T.; Minamikawa, J.-i. Progress in arylpiperazine synthesis by the catalytic amination reaction. *Bioorg. Med. Chem.* **2002**, 10, 4023–4027.
- (10) (a) Pilla, M.; Perachon, S.; Sautel, F.; Garrido, F.; Mann, A.; Wermuth, C. G.; Schwartz, J.-C.; Everitt, B. J.; Sokoloff, P. Selective inhibition of cocaine-seeking behaviour by a partial dopamine D3 receptor agonist. *Nature* **1999**, 400, 371–375. (b) Bezaud, E.; Ferry, S.; Mach, U.; Stark, H.; Leriche, L.; Boraud, T.; Gross, C.; Sokoloff, P. Attenuation of levodopa-induced dyskinesia by normalizing dopamine D3 receptor function. *Nat. Med.* **2003**, 9, 762–767.
- (11) Hayes, G.; Biden, T. J.; Selbie, L. A.; Shine, J. Structural subtypes of the dopamine D2 receptor are functionally distinct: expression of the cloned D2A and D2B subtypes in a heterologous cell line. *Mol. Endocrinol.* **1992**, 6, 920–926.
- (12) Sokoloff, P.; Andrieux, M.; Besançon, R.; Pilon, C.; Martres, M.-P.; Giros, B.; Schwartz, J.-C. Pharmacology of human dopamine D3 receptor expressed in a mammalian cell line: comparison with D2 receptor. *Eur. J. Pharmacol.* **1992**, 225, 331–337.
- (13) Asghari, V.; Sanyal, S.; Buchwaldt, S.; Paterson, A.; Jovanovic, V.; Van Tol, H. H. M. Modulation of intracellular cyclic AMP levels by different human dopamine D4 receptor variants. *J. Neurochem.* **1995**, 65, 1157–1165.
- (14) (a) Mierau, J.; Schneider, F. J.; Ensinger, H. A.; Chio, C. L.; Lajiness, M. E.; Huff, R. M. Pramipexole binding and activation of cloned and expressed dopamine D2, D3 and D4 receptors. *Eur. J. Pharmacol.* **1995**, 290, 29–36. (b) Hübner, H.; Kraxner, J.; Gmeiner, P. Cyanoindole derivatives as highly selective dopamine D4 receptor partial agonists: solid-phase synthesis, binding assays, and functional experiments. *J. Med. Chem.* **2000**, 43, 4563–4569.
- (15) Chio, C.; Lajiness, M. E.; Huff, R. M. Activation of heterologously expressed D3 dopamine receptors: comparison with D2 dopamine receptors. *Mol. Pharmacol.* **1994**, 45, 51–60.
- (16) Clark, T.; Alex, A.; Beck, B.; Chandrasekar, J.; Gedeck, P.; Horn, A.; Hutten, M.; Martin, B.; Rauhut, G.; Sauer, W.; Schindler, T.; Steinke, T. *VAMP 7.0 Program Package*; Oxford Molecular Group Plc.: Oxford, U.K., 1998.
- (17) Frisch, M. J.; Trucks, G. W.; Schlegel, H. B.; Scuseria, G. E.; Robb, M. A.; Cheeseman, J. R.; Zakrzewski, V. G.; Montgomery, J. A., Jr.; Stratmann, R. E.; Burant, J. C.; Dapprich, S.; Millam, J. M.; Daniels, A. D.; Kudin, K. N.; Strain, M. C.; Farkas, O.; Tomasi, J.; Barone, V.; Cossi, M.; Cammi, R.; Mennucci, B.; Pomelli, C.; Adamo, C.; Clifford, S.; Ochterski, J.; Petersson, G. A.; Ayala, P. Y.; Cui, Q.; Morokuma, K.; Malick, D. K.; Rabuck, A. D.; Raghavachari, K.; Foresman, J. B.; Cioslowski, J.; Ortiz, J. V.; Stefanov, B. B.; Liu, G.; Liashenko, A.; Piskorz, P.; Komaromi, I.; Gomperts, R.; Martin, R. L.; Fox, D. J.; Keith, T.; Al-Laham, M. A.; Peng, C. Y.; Nanayakkara, A.; Gonzalez, C.; Challacombe, M.; Gill, P. M. W.; Johnson, B. G.; Chen, W.; Wong, M. W.; Andres, J. L.; Head-Gordon, M.; Replogle, E. S.; Pople, J. A. *Gaussian 98*, revision A.7; Gaussian, Inc.: Pittsburgh, PA, 1998.
- (18) Lenz, C.; Boeckler, F.; Hübner, H.; Gmeiner, P. Analogues of FAUC 73 revealing new insights into the structural requirements of nonaromatic dopamine D3 receptor agonists. *Bioorg. Med. Chem.* **2004**, 12, 113–117.
- (19) Lenz, C.; Boeckler, F.; Hübner, H.; Gmeiner, P. Fancy bioisosteres: synthesis, SAR, and pharmacological investigations of novel non-aromatic dopamine D3 receptor ligands. *Bioorg. Med. Chem.* **2005**, 13, 4434–4442.
- (20) Wolinski, K.; Hinton, J. F.; Pulay, P. Efficient implementation of the gauge-independent atomic orbital method for NMR chemical shift calculations. *J. Am. Chem. Soc.* **1990**, 112, 8251–8260.
- (21) Meyer, E. A.; Castellano, R. K.; Diederich, F. Interactions with Aromatic Rings in Chemical and Biological Recognition. *Angew. Chem., Int. Ed.* **2003**, 42, 1210–1250.
- (22) Allen, F. H. The Cambridge Structural Database: a quarter of a million crystal structures and rising. *Acta Crystallogr., Sect. B* **2002**, 58, 380–388.
- (23) *PC Spartan Plus*, version 1.5; Wave Function, Inc.: Irvine, CA, 1998.
- (24) *SYBYL6.9*; Tripos Inc.: St. Louis, MO, 2003.
- (25) Cram, D. J.; Allinger, N. L. Macro Rings. XII. Stereochemical consequences of steric compression in the smallest paracyclophane. *J. Am. Chem. Soc.* **1955**, 77, 6289–6294.
- (26) Cram, D. J.; Day, A. C. Macro Rings. XXXI. Quinone derived from [2.2]paracyclophane, an intramolecular-molecular complex. *J. Org. Chem.* **1966**, 31, 1227–1232.
- (27) Falk, H.; Reich-Rohrwig, P.; Schlogl, K. Absolute configuration and circular dichroism of optically active [2.2]paracyclophane derivatives. *Tetrahedron* **1970**, 26, 511–527.
- (28) Lowry, O. H.; Rosebrough, N. J.; Farr, A. L.; Randall, R. J. Protein measurement with the folin phenol reagent. *J. Biol. Chem.* **1951**, 193, 265–275.
- (29) Cheng, Y. C.; Prusoff, W. H. Relationship between the inhibition constant (K_i) and the concentration of inhibitor which causes 50% inhibition (IC_{50}) of an enzymatic reaction. *Biochem. Pharmacol.* **1973**, 22, 3099–3108.